Chapter 8
Surface Engineering for Biotribological Application

D.V. Shtansky and Manish Roy

8.1 Introduction

Advances in medical science and development in biomedical materials have led to a remarkable increase in ageing population and improvement of quality of life. Monitoring of friction and wear in human body has played a very significant role in enhancing human lifespan. Several organs, joints and critical parts of human body wear out and need to be replaced. Friction and wear play important role in several cardiovascular devices. Heart disease is one of the most common diseases requiring replacement of heart valve. Artificial heart valves are used to replace damaged or diseased natural valves resulting in significant improvement of life span and quality of life. These valves are generally made of pyrolytic carbon (PyC). However, this material is brittle and has low blood compatibility. Consequently, the patients suffer from thrombosis and require taking anti-coagulation medicine which has side effects. Synthetic vascular grafts are used to repair weakened blood vessels to bypass blockages has resulted in enhanced blood flow to severely ischemic organs and limbs. In order to improve the pumping function of the heart, intra-aortic balloon pump, ventricular assist device, total implantable artificial heart, etc. are being used. Pacemakers and automatic internal defibrillators are widely used to over ride or correct aberrant, life-threatening cardiac arrhythmias. All these devices are subjected to wear and tear during implanting or during operation. In addition, life threatening occlusive diseases of the arteries is treated with implantation of stents. It is a device which is inserted into the body passages using catheter to maintain the flow of blood, urine, bile or air. It is important to minimise the friction

D.V. Shtansky (✉)
National University of Science and Technology "MISIS", Leninsky pr. 4, Moscow 119049, Russia
e-mail: Shtansky@shs.misis.ru

M. Roy
Defence Metallurgical Research Laboratory, Kanchanbagh, Hyderabad 500058, Andhra Pradesh, India

M. Roy (ed.), *Surface Engineering for Enhanced Performance against Wear*,
DOI 10.1007/978-3-7091-0101-8_8,

during insertion and removal of stents in order to minimise damages of tissue. There are several approaches to minimise such friction. Surface coating with self-lubrication layer is one measure which has become very popular in recent times. However, such treatment suffers from the drawbacks of thrombotic occlusion/stenosis and restenosis [1–3] due to platelet activation, etc. [4]. Similarly, thromboembolism is another problem for management of implanted mechanical heart valve prosthesis [5]. Further, medical implants can fail due to wear, fatigue, chemical degradation, infection, etc. leading to osteolysis, loosening.

Two well-known fields for biomedical implants are orthopaedics and dentistry. Among clinical orthopaedics implant, total joint replacements of hip, knee, shoulder and ankle have received maximum attention in recent time. These joints operate by low-friction articular cartilage-bearing surfaces, which are conforming and self-regenerating [6, 7]. When natural joints are severely damaged, e.g. due to osteoarthritis, they are replaced by implants. In total joint replacement, a cup is fixed in the acetabulum against which is articulated a femoral head. The implant surface must be tolerant to dynamic loading to which it is subjected during usage and should have ability for long-term exposure to biological interaction with surrounding tissue. Similarly, dental implant abutment screws joint tend to loosen and undergo wear and friction. However, prolong usage of implanted joints generates wear debris which results in formation of granulomatous inflammatory response of the periprosthetic tissues (osteolysis). The wear debris simulates formation of multinucleated giant cells, whereas small particles are phagocytosed by macrophases. These small particles produce several osteolytic cytokines and mediators that change the osteoclast and osteoblast activities. This causes bone resorption and subsequent implant loosening. Thus further development of joint replacement is concerned with durability of the implant.

While metals and alloys meet many requirements of biomaterials, the interfacial bonding between the metallic surface and the surrounding bone is poor or does not exist at all [8]. Ceramics are potential bioactive implant materials. However, it should be noted that the clinical application of bioactive ceramics in high-load bone implants is limited because of its low fracture toughness. An effective way to promote the formation of bone-like layer on the implant surface is the deposition of bioactive or biotolerant coating. Further, it is noted that application of various coating enhances wear and friction behaviour, biocompatibility, hemocompatibility, etc. of metallic implant. Thus, the aim of this chapter is to examine the present state of art of different surface modification techniques available to improve the performances of physiological implants against tribological degradations.

8.2 Wear of Implants

Knee, shoulder and hip joints involve a sliding contact between the femoral component and the tibial or acetabular component during the motion of the human body. As a result, the metallic components of the artificial joint are

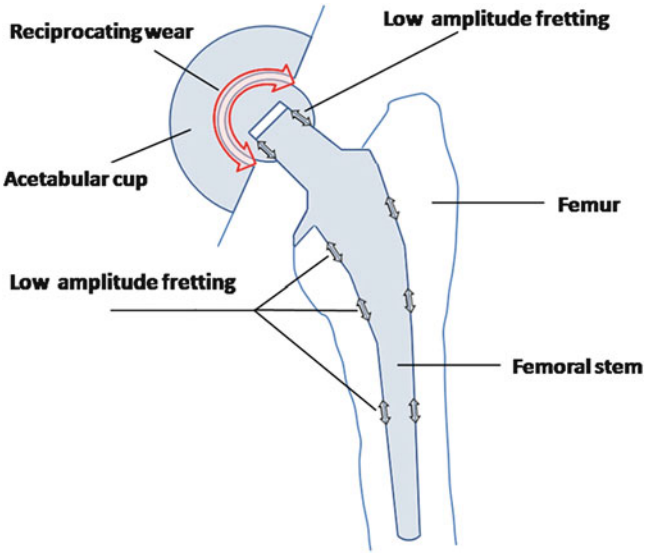

Fig. 8.1 A schematic representation of a total hip joint replacement prosthesis showing the types of motion and surface degradation mechanisms of the implant's metallic components

susceptible to sliding wear as shown in Fig. 8.1. Fretting wear is a particular form of wear involving a small amplitude relative displacement [9]. In the particular case of orthopaedic implants, micro-motions are known to occur at points of fixation between the different components [10], while corrosion is caused by the body fluid which contains various inorganic and organic ions and molecules [11] (see Fig. 8.1). Fretting has been identified at the neck/head contact and at the stem/bone interface of modular hip joints and at the screw head/plate junction of fixation plates [12]. In contrast to sliding, during fretting, a considerable part of the displacement may be accommodated in the contact by elastic deformation and thus the elastic properties of protective coatings can affect the implants behaviour and functionality. Furthermore, due to the closed geometry of the contact, debris is easily trapped and thus the behaviour of the third body is critical.

As mentioned earlier, stents is a device which is inserted into the body passages using catheter to maintain the flow of blood, urine, bile or air. It is important to control the friction during insertion and removal of stents in order to minimise damages of tissue. This problem is counter either by using hydrophobic polymer or by introducing special lubricant known as RotaGlide™ in to the guiding catheter [13]. Several cardiovascular devices, such as heart valves, vascular grafts, intra-aortic balloon pump, etc., are subjected to wear and tear during implanting or during operation.

Methods of joining prosthesis components in dental implant systems are very important to prevent implant/abutment rotation. Figure 8.2 shows a dental implant system. If the abutment screw does not remain properly affixed during masticator loading, it is necessary to retighten the screw to prevent prosthesis rotation, thus increasing the cost of the treatment and the patient discomfort. Although bolt joints have been extensively studied, they are a very complex structure and their

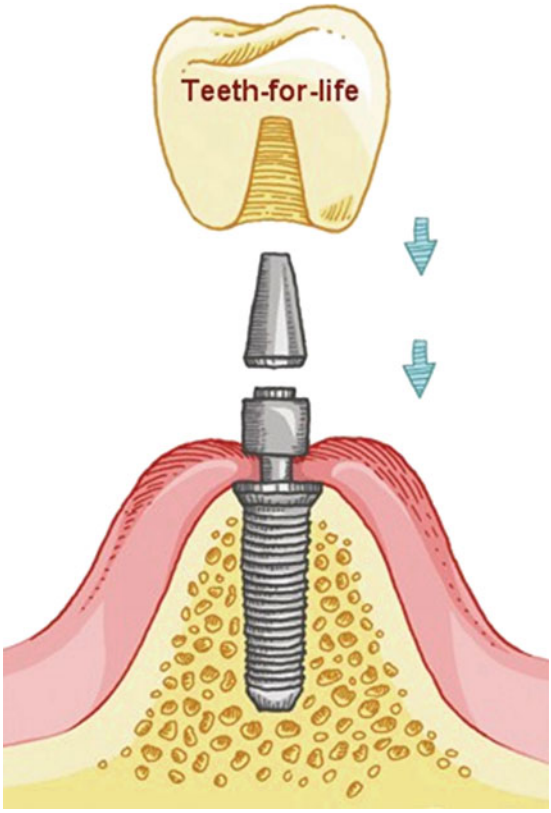

Fig. 8.2 The dental implant system

behaviour is not well known. They are not very stable and can flex, shift and relax under environmental changes and/or variations in external load. The torque applied to the screw joint during tightening is not entirely translated into screw preload since part of this torque is expended to overcome friction. About 50 % of the energy transmitted by torque tightening is expended to overcome the friction between the abutment screw head and the abutment-seating surface. About 40 % of the applied torque is used to overcome thread friction and only 10 % produces the screw tension. As a result the effective joint preload is smaller than the applied torque. In addition, even in properly joined implant various parts of dental implants are subjected to frictional degradation during mastication.

8.3 Classification of Coatings for Biomedical Application

Coating for biomedical application can be classified depending on their biocompatibility and tissue response. They can be described as biotolerant, bioinert and bioactive. Biotolerant coatings release materials which are non-toxic and they may cause benign tissue reactions such as formation of a fibrous connective tissue

capsules or weak immune reaction leading to formation of giant cells or phagocytes. These coatings are characterised by development of fibrous tissues around the coatings [14, 15]. Stainless steel coatings deposited by thermal spraying technique or bone cement coatings containing polymethylmethacrylate (PMMA) can be categorised under this head. The interaction between the coating and the surrounding tissue is minimum for the bioinert coating. These coatings do not show any positive interaction with living tissues [16]. Various titanium-based coatings, ceramic coatings such as alumina, zirconia, titania, etc. and some polymeric coating are bioinert coatings. Those coatings which develop positive bone response and cause bone growth and regeneration in vivo site of application are known as bioactive coatings. They can bond to bone by formation of bone-like apatite layer on the surface of implants through chemical bonding along the bone–implant interface. These layers are essentially bone-like carbonate appetite layer that is chemically and crystallographically equivalent to the mineral phase in nature bone [17]. These coatings can act as scaffolding for bone cell migration and proliferation leading to new bone growth. Therefore, it is believed that a coating should contain HAP ($Ca_{10}(PO_4)_6(OH)_2$) components, such as Ca, P and O for it to have apatite nucleation ability. It has been shown that bioactive glasses and certain ceramics release Ca^{2+} ions through an exchange with protons of the body fluids when implanted into bone [18]. Nevertheless, evaluation of various bioceramics has shown that even P_2O_5-free CaO–SiO_2 and CaO- and P_2O_5-free Na_2O–SiO_2 glasses can form apatite in simulated body fluid [19]. It has been also shown that apatite nucleation is induced by hydroxyl functional groups on the bioactive coatings surface [19, 20]. The body environment of these functional groups assumes a negative surface charge [19] that stimulates apatite growth. There interfaces permit transmission of compressive, tensile and shear stresses. Synthetic hydroxyapatite (HA), calcium phosphate and bioglass coatings can be considered as bioactive coatings.

8.3.1 Bioactive Coatings

As discussed earlier that the effective way to promote the formation of bone-like layer on the implant surface is to modify the surface with bioactive layer. One way to do that is to deposit multifunctional bioactive coating. Ceramics coatings, such as ZrO_2, TiN, TiO_2, SiO_2 and SiC are potential coatings on implant surface. Zirconia (ZrO_2) ceramics and its composites possess excellent mechanical properties. These ceramics were evaluated as biomaterials in the late 1960s and are used for orthopaedic implants as ball heads in artificial hip joints [21, 22]. However, ZrO_2 does not bond directly to bone. TiN coatings because of its excellent combination of useful properties such as high hardness, wear and corrosion resistance and biocompatibility have a wide range of applications such as dental prosthesis, materials for hip joint and heart valve replacements [23, 24]. TiN [25, 26] and TiO_2 [27] films have shown to possess excellent hemocompatibility. Further discussion on

biotribology of TiN, ZrO_2 and TiO_2 coatings is carried out in subsequent section. SiO_2 and TiO_2 ceramics induce apatite formation due to a negative surface charge under physiological pH [28]. Bioactive silicate glasses can form a bond with bone tissue [29] and have been used in a number of clinical applications [30]. Amorphous SiC alloys have been employed to enhance the biocompatibility of artificial heart valves [31].

Shtansky et al. developed multifunctional bioactive nanostructured films (MuBiNaFs) and evaluated them as perspective biomaterials to be used in load-bearing medical applications [32, 33]. A comparative investigation of MuBiNaFs based on the systems Ti–Ca–C–O–(N), Ti–Zr–C–O–(N), Ti–Si–Zr–O–(N) and Ti–Nb–C–(N) is carried out by them [34]. $TiC_{0.5}$ + 10 % CaO, $TiC_{0.5}$ + 20 % CaO, $TiC_{0.5}$ + 10 % ZrO_2, $TiC_{0.5}$ + 20 % ZrO_2, Ti_5Si_3 + 10 % ZrO_2, $TiC_{0.5}$ + 10 % Nb_2C and $TiC_{0.5}$ + 30 % Nb_2C composite targets were manufactured by means of self-propagating high-temperature synthesis. Subsequently above-mentioned films were deposited by DC magnetron sputtering in an atmosphere of argon or in a gaseous mixture of argon and nitrogen. The films were characterised in terms of their structure, chemical composition, surface topography, hardness, elastic modulus, elastic recovery, surface charge, friction coefficient and wear rate. The biocompatibility of the films was evaluated by both in vitro and in vivo experiments. The transmission electron microscopy image of Ti–Si–Zr–O–N film and Ti–Nb–C–N film along with their corresponding diffraction pattern is presented in Fig. 8.3. Ti–Si–Zr–O–N films deposited in a gaseous mixture of Ar + N_2 exhibits a cubic structure (lattice type B1) having nanocrystalline grains. Ti–Nb–C–N film also displays nanocrystalline structure with the grain size $d < 50$ nm. The films deposited under optimal conditions showed high hardness in the range of 30–37 GPa, significant reduced Young's modulus, low friction coefficient down to 0.1–0.2 and low wear rate in comparison with conventional magnetron-sputtered TiC and TiN films. The friction coefficient of a series of films deposited on Ti base alloy is presented in Fig. 8.4 [32]. These films were tested against WC–Co ball. All films have very low friction coefficient, although addition of nitrogen does not alter it significantly. Similarly wear rate of a series of MuBiNaFs deposited on hard metal is illustrated in the form of bar diagram in Fig. 8.5 [32]. Except Ti–Si–Zr–O–N film, other films have reasonably low wear rate. High wear rate of Ti–Si–Zr–O–N film is related to its high friction coefficient. The predominant wear mechanism is found to be abrasion. The morphology of worn surfaces of Ti–Ca–P–C–O film and Ti–Ca–C–O film after approximately 14,000 cycles is presented in Fig. 8.6a, b. Although abrasive wear proceeded mainly by plastic deformation mechanism, it also occurred through brittle fracture when a critical load was exceeded. It can be seen that the film failure started from the generation of a few chevron cracks within the wear track leading to changes in stress distribution and increase in local sliding friction force. This resulted in fast ductile perforation of the film due to the cyclic loading. Although abrasion was a dominant wear mechanism, contribution of tribochemical reaction and corrosive wear was also evident.

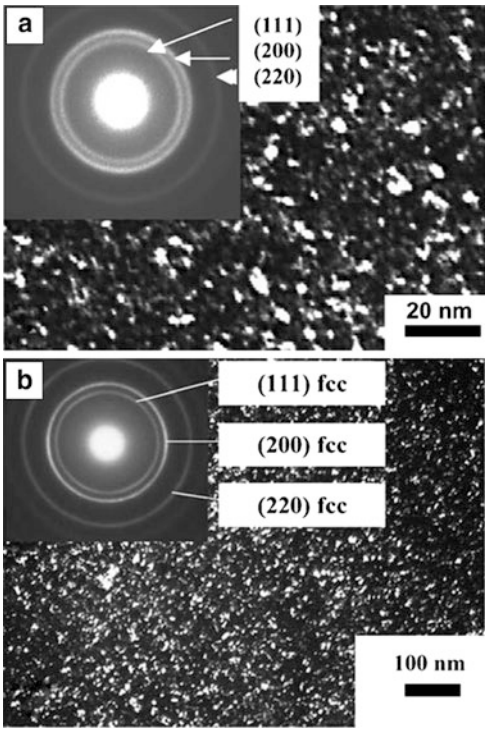

Fig. 8.3 The transmission electron microscopy images of (**a**) Ti–Si–Zr–O–N film and (**b**) Ti–Nb–C–N film along with their corresponding diffraction patterns [32]

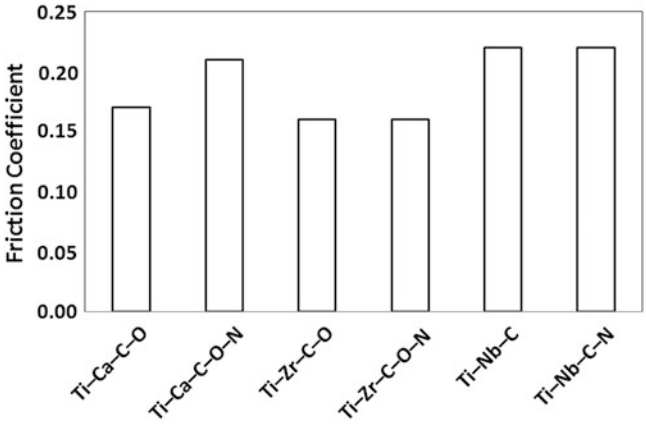

Fig. 8.4 The friction coefficient of a series of multicomponent bioactive Ti-based film deposited on Ti base alloy using dc magnetron sputtering [32]

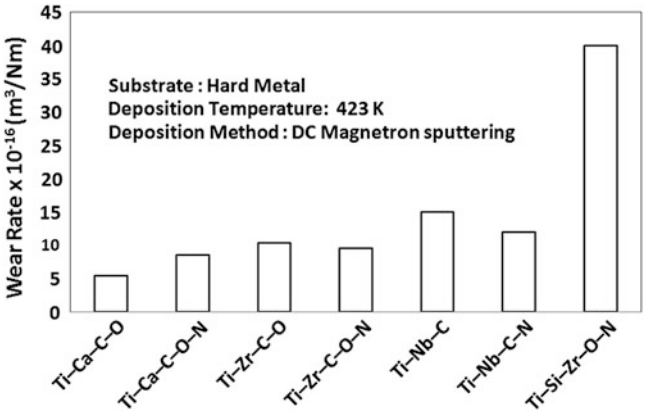

Fig. 8.5 Wear rate of a series of multicomponent bioactive Ti-based films deposited on hard metal substrates [32]

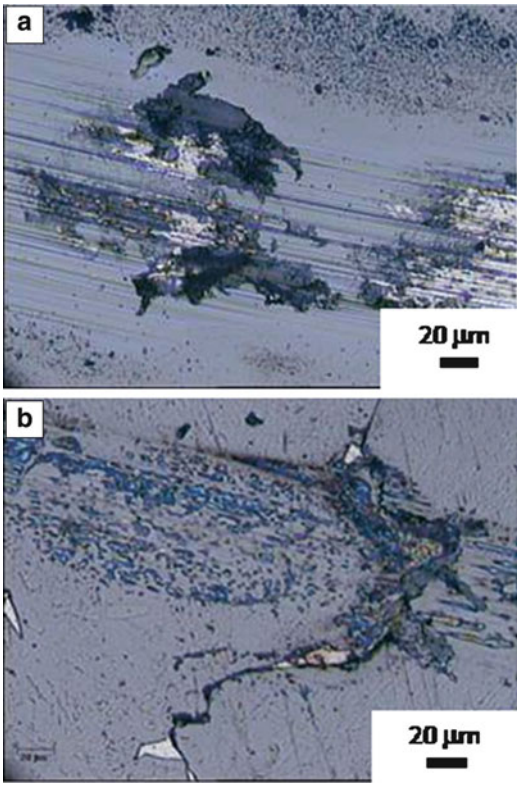

Fig. 8.6 SEM images showing the morphology of worn surfaces of (a) Ti–Ca–P–C–O film and (b) Ti–Ca–C–O films after approximately 14,000 cycles [39]

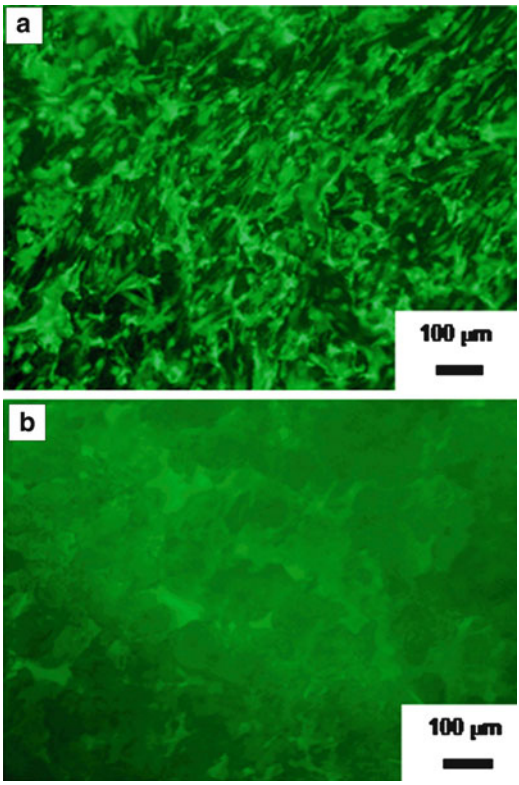

Fig. 8.7 The fluorescence microscopy images showing the high population of fibroblast cells on the surface of PTFE coated with the TiCaPCON film and a low cell density on the uncoated PTFE surface [38]

More recently, Ta- and Si-doped Ti–Ca–P–C–O–N films have been developed [35, 36]. The films possessed a nanocomposite structure with various functional groups on the film surface that stimulate accelerated osseointegration. For instance, the Si-doped Ti–Ca–P–C–O–(N) films sputter-deposited using composite $TiC_{0.5}$ + CaO + Si and $TiC_{0.5}$ + CaO + Si_3N_4 targets consisted of TiC(N) as a main phase with a minor amount of TiO_x, SiN_x, SiO_x, SiC and CaO phases which were probably mainly in an amorphous state at the grain boundaries and COO– groups on the film surface. Excess carbon atoms precipitated in the Ti–Si–Ca–P–C–O–N film (N-free target) in a DLC form. The excellent biocompatibility of these films were characterised by investigation using fluorescence microscopy which identified the high population of fibroblast cells on the surface of PTFE coated with the TiCaPCON film, while a low cell density was observed on the uncoated PTFE surface as shown in Fig. 8.7a, b. The Ta-doped Ti–Ca–(P)–C–O–(N) films deposited in argon consisted of (Ti,Ta)C, Ti_xO_y and CaO phases in an amorphous matrix with P–O, C–O and O–H bonding. The films reactively sputtered in Ar + N_2 atmosphere exhibited (Ti,Ta)(C, N), Ti_xO_y and CaO phases, diamond-like carbon, *bcc* Ta and indications of P–O bonding. A typical XPS spectra obtained from Ti–Ta–Ca–P–C–O film is presented in Fig. 8.8. Main peak is at 454.6 and 460.7 eV confirms presence of TiC. Existence of TiC peak is also confirmed by characteristics band at 281.9 eV. A weak peak at

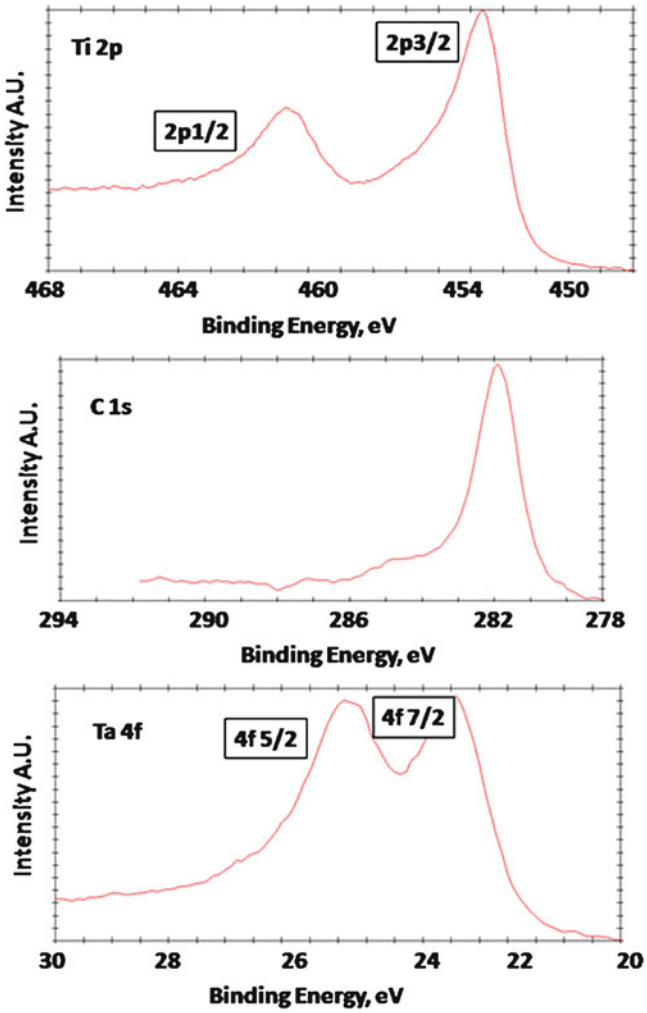

Fig. 8.8 The typical XPS spectra obtained from Ti–Ta–Ca–P–C–O film [35]

286 eV suggests presence of C–C. The tantalum peak at 22.75 eV can be attributed to Ta carbide.

A comparison of properties of the MuBiNaFs with the properties of bulk materials (Ti-, Ni- and Co-based alloys, stainless steel, ceramics) and thin films produced by alternative methods shows a noticeable advantage from the viewpoint of the whole combination of physical, mechanical, tribological, and biological properties. The MuBiNaFs are characterised by high hardness 25–40 GPa, combined with a high percentage of elastic recovery (up to 75 %) and reduced Young's modulus of 230–350 GPa, which is lower than those of bulk ceramics (TiN—440 GPa, TiC—480 GPa, SiC—450 GPa and Al_2O_3—390 GPa) and close to the

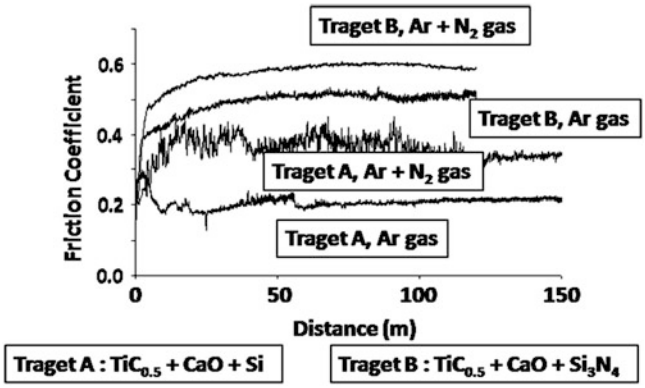

Fig. 8.9 Typical friction curve of MuBiNaF coatings [36]

modulus of stainless steel (200 GPa) and Ti (120 GPa). The benefits of a moderately low Young's modulus in bioimplant applications are well known: better transfer of functional loads to bone and reduced interfacial stresses between the film and substrate materials. The MuBiNaFs also showed high resistance to plastic deformation (up to 0.9 GPa) and long elastic strain to failure, which was previously reported as a good indicator of high film durability and wear resistance [37]. Other mechanical characteristics include a high fatigue limit of 350 MPa (MuBiNaFs on a Grade 4 Ti substrate), high adhesion strength (up to 50 N) and excellent impact resistance. The MuBiNaFs demonstrated hydrophilic nature, negative surface charge at pH 5–8.5, positive values of corrosion potential with low current density under various biological solutions, bioactivity, biocompatibility and non-toxicity.

The Ta-doped MuBiNaFs tested against Al_2O_3 ball showed low friction coefficient down to 0.2–0.25 and wear rate of (0.7–6.8) $\times$ 10^{-6} mm^3 N^{-1} m^{-1} both in air and under physiological solution and this is two orders of magnitude lower than that of Ti [35]. Depending on the target used, a large difference in the friction coefficient of Ti–Si–Ca–C–O–N films was reported [36]. Under physiological solution (normal saline), the films deposited using the $TiC_{0.5}$ + CaO + Si target displayed a friction coefficient within the range of 0.2–0.33, whereas the films deposited using the $TiC_{0.5}$ + CaO + Si_3N_4 target had a higher friction coefficient of about 0.5–0.55. Typical friction curve of these coatings is illustrated in Fig. 8.9. A transfer layer observed in the bottom of wear track (due to the wear of the ball) indicated adhesion wear as the dominant wear mechanism. The Ti–Si–Ca–C–O–N films tested in a Dulbecko modified Eagle medium with Fetal calf serum (DMEM + FCS) showed low values of the friction coefficient and a wear rate down to 0.15 and (0.9–1.5) $\times$ 10^{-6} mm^3 N^{-1} m^{-1}, respectively. This finding can be explained by an increase of the solution viscosity which results in an increase of the hydrodynamic component of the lubrication. The wear track was relatively smooth and free from the adherent or transferred material. Thus the dominant wear mechanism changed from adhesion to abrasive wear when the samples were transferred from

Fig. 8.10 Images of hip implants (CONMET, Russia) coated with MuBiNaF (MISIS, Russia)

a physiological solution to a DMEM + FCS medium. Image of MuBiNaFs-coated hip implants is presented in Fig. 8.10.

Shtansky et al. [38] showed that the modification of the PTFE surface by the deposition of TiCaPCON films with and without stem cells was an effective way to improve the chemical and mechanical characteristics of polymer implants and provided them with a high osseointegration potential. The friction behaviour of the TiCaPCON films was examined in different environments. The friction coefficient μ of PTFE substrate tested under physiological solution displayed initial maxima followed by a drop to a value about 0.035 after a short run-in period about 10 m. The somewhat high value of μ at the beginning of the test can be ascribed to a high PTFE surface roughness. The steady state friction coefficient of the TiCaPCON film deposited on PTFE was 0.13. This value was lower compared with 0.2–0.24 reported for the TiCaPCON films deposited on the Al_2O_3 substrate and tested under similar conditions [39]. The use of a DMEM + FCS medium did not change the steady-state friction coefficient of the TiCaPCON films which reached the value of 0.13 after the sliding distance of 25 m. The friction profile of the TiCaPCON films in DMEM + FCS was smoother compared with that in normal saline but exhibited small fluctuations (± 0.01).

Park et al. [40] examined the characteristics of calcium phosphate coatings deposited by electrodeposition on as-received Ti and titanium substrate treated with H_2O_2 in a modified simulated body fluid (SBF). A porous coating comprising of mainly hydroxyapatite (HA) was formed on the H_2O_2-treated titanium substrate. During immersion in the SBF, this coating was transformed into carbonate and calcium-deficient HA layers with a bone-like crystallinity. Interestingly, uniformed coating containing amorphous calcium phosphate formed on the untreated titanium substrate was transformed into poorly crystalline HA during immersion in the SBF. This difference was attributed to the increased surface area of the titanium substrate due to the H_2O_2 treatment and to the release of the OH_ ions from this modified surface during electrodeposition. Thus, H_2O_2 treatment prior to electrodeposition is an effective method for preparing a potentially bioactive calcium phosphate coating by electrodeposition.

The widely studied bioactive coating is a calcium-phosphate-based material hydroxyapatite (HA) having formula $Ca_{10}(PO_4)_6(OH)_2$ [41]. HA is one of the

most attractive materials for human hard tissue implants because of its close resemblance to chemical composition (Ca/P ratio) of teeth and bones [42, 43]. This coating accelerates the bone growth process in the vicinity of the prosthesis [44–49]. This material has been clinically applied as a coating on bioinert metallic implants [50]. The excellent biocompatibility and bioactivity for skeletal and dental Ti implants coated with HA may be due to the OH, and O concentrations decrease with the distance from the surface of HA coatings reaching the minimum at the interface between HA and Ti alloys [51]. HA coatings on a Ti–6Al–4V substrate obtained by plasma spraying are found to increase both resistances to elastic and plastic deformation especially after a heat treatment [52]. However, such coatings have no effects on strain hardening behaviour. The coating also has improved resistance to coating/substrate separation [53]. The fracture toughness of the coating is about 1 MPa $m^{1/2}$and it has low fatigue resistance [54, 55]. In order to achieve the mechanical characteristics needed for biomedical applications, blending with a tough phase is essential. β-Ti alloy, yttria-stabilized zirconia (YSZ), Ni_3Al and Al_2O_3 ceramics have been considered good candidates as the reinforcing phases [56–60]. These coatings can be applied by a wide range of surface deposition techniques, such as high velocity oxy-fuel spraying (HVOF), plasma spraying, pulsed laser ablation, sputtering, electrophoretic deposition, sol–gel and conventional ceramic processes that involve pressing and sintering [61–66]. The thickness of HA coating can be controlled between 40 and 400 μm [66]. Different phases in HA coatings exhibit different solubilities and dissolution behaviours. Amorphous HA has been found to be more soluble than crystalline HA [67–69] in aqueous solutions. HA is thermodynamically unstable at high temperatures and when used in plasma spraying, it promotes the formation of CaO which reacts with water and has a high solubility in body fluids. High temperature deposition processes are also responsible for the formation of amorphous phases that reduce the coating–metal interfacial strength. Therefore recent developments have concentrated on improving coating stability and adhesion. A controlled atmosphere plasma spraying (CAPS) system is found to be useful for controlling the degree of melting of the HA powder, enabling coatings of tailored microstructure to be produced [70]. Yttria-stabilized zirconia incorporated into HA coating results in composite coatings containing more unmelted particles and greater porosity [71]. ZrO_2 reacts with CaO to form $CaZrO_3$. This has been achieved by thermal treatment of the coating after deposition. A post-heat treatment promotes the complete crystallisation of the amorphous calcium phosphate and this results in much improved adhesion [72]. A recent study [73] addressed the poor bond strength between HA coating and the metal substrate by considering the mismatch in physical and chemical properties between the ceramic coating and metal. The large difference in thermal expansion coefficient and rapid cooling of the plasma-sprayed droplets results in residual stress in the coating that is responsible for compromise of adhesion. To eliminate the delamination problem of HA coatings from their substrate [74], a bond coating, dicalcium silicate, is applied using the plasma coating technique. The plasma-sprayed dicalcium silicate, Ca_2SiO_4, is a bond coat for improving the bonding of HA coatings on Ti alloys substrates [75]. Overall, HA coatings can improve the adhesion and fixation of an implant device. A

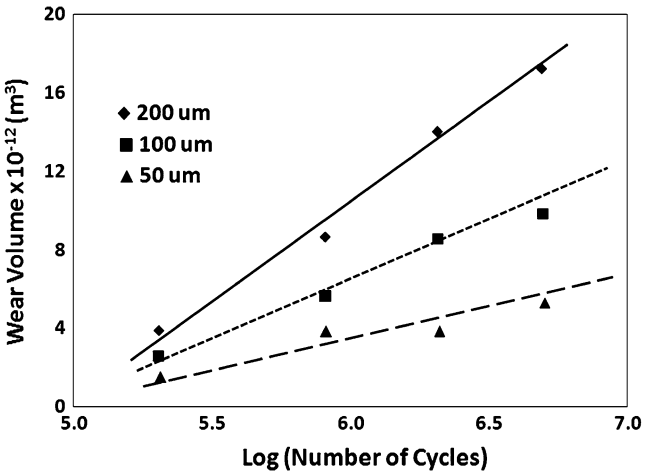

Fig. 8.11 The fretting wear of HA coating under lubricated conditions at the amplitudes of 50, 100, and 200 μm as a function of fretting cycles and normal loads of 10 N [76]

mechanical interlocking of implant with bone can eliminate problems associated with micromotion, i.e. loosening. Consequently coated implants can be recommended for applications involving younger or more active patients.

Fu et al. [76] studied the fretting wear behaviour of plasma-sprayed hydroxyapatite HA coatings lubricated with bovine albumin solution as a function of normal load, oscillatory cycle and slip amplitude. Wear mechanisms, wear volume and coefficient of friction of HA coating under lubricated fretting conditions were investigated. Fretting wear mechanisms of plasma-sprayed HA coatings under lubricated conditions were found to be mainly delamination, pitting and abrasive wear. Figure 8.11 shows the fretting wear volume of HA coating under lubricated conditions at the amplitudes of 50, 100 and 200 μm as a function of fretting cycles and normal loads of 10 N. The wear volume decreases with decrease in amplitude of cycles. Bovine albumin is an effective lubrication during fretting as shown in Fig. 8.12. It is also clear from Fig. 8.12 that hot isostatic pressing (HIP) treatment densified the coating structure, decreased the generation of fretting wear debris and improved the fretting wear resistance and hence, it could be used as a post-treatment method for as-sprayed HA coating. Although significant work is done on tribocorrosion behaviour of Ti base alloys under fretting condition [77, 78], fretting corrosion of bioactive coating has not been reported so far.

8.3.2 Bioinert Coating

Ti-based surface can be considered to be bioinert. These alloys exhibit excellent corrosion resistance in physiological solution [79]. Surface modification of Ti-

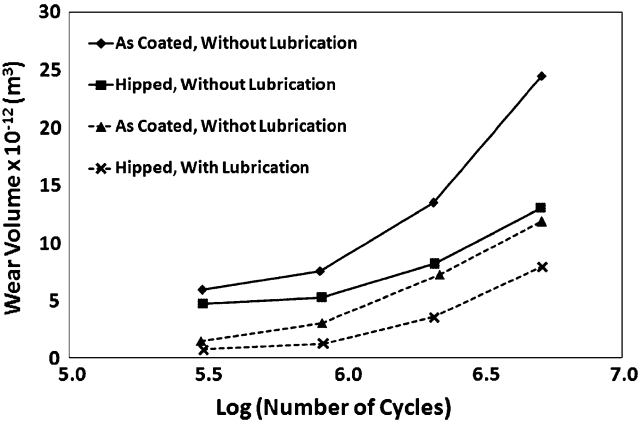

Fig. 8.12 The fretting wear of HA coating under lubricated conditions showing hot isostatic pressing (HIP) treatment improves wear performance [76]

based joint implant is carried out by employing laser-engineered net shape processing [80, 81]. In general, Ti-based alloys have poor tribological properties [82, 83]. The tribological properties of TiB/Ti–6Al–4V metal matrix layer fabricated by laser cladding and laser melting injection exhibited markedly improve wear performances [84]. Wear behaviour was studied for the composite layer laser processes using a mixture of 51 wt.% Ti + 35 wt.% b + 7 wt.% Zr + 5 wt.% Ta and 2 wt.% B. Wear studies indicate when Si_3N_4 is used as counterbody, TiB precipitates are pulled out resulting in higher friction coefficient and higher wear rate. If the counter body is 440C stainless steel ball, a drastic improvement of friction coefficient and wear rate is noted.

Nanocrystalline diamond coatings (NCD) are gaining increasing interest as serious candidate materials for high performance engineering surfaces in mechanical and tribological applications, due to their intrinsic smoothness combined with most of the outstanding properties of natural single-crystal diamond [85, 86]. High resolution transmission electron micrograph of NCD film is presented in Fig. 8.13 [86]. Small grains of the order of 10–15 nm can be observed. A typical diffraction pattern obtained from EELS is given in Fig. 8.14. The deposition of nanocrystalline diamond (NCD) coatings on load bearing surfaces can improve their wear resistance and life span. NCD films possess outstanding physical and tribomechanical properties such as very low friction response and high wear resistance. In addition, their biocompatible character makes them an ideal choice for biotribological purposes. Reports of works on NCD-coated metal alloys for implants such as hip, knee and temporomandibular joints, with the purpose of wear resistance improvement are found in the literature [87–89].

A nanocrystalline diamond (NCD)-coated Si_3N_4–bioglass composite, with potential use for hip and knee joint implants, was tribologically tested in simulated physiological fluids by Amaral et al. [90]. NCD was deposited using a hot-filament chemical vapour deposition (HFCVD) apparatus in an Ar–H_2–CH_4 gas mixture.

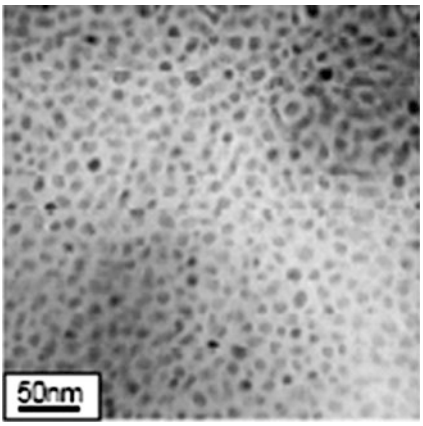

Fig. 8.13 TEM image of nanocrystalline diamond film [86]

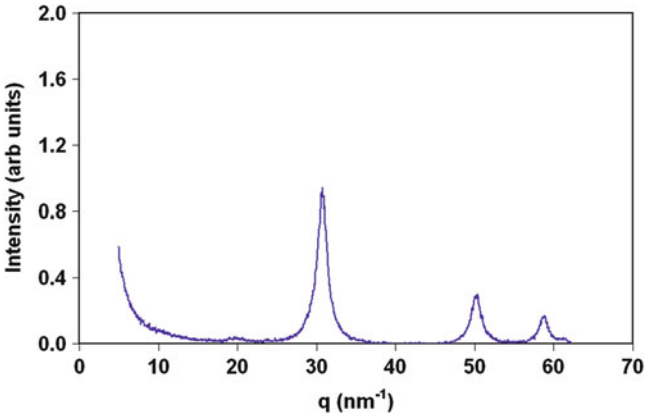

Fig. 8.14 A typical diffraction pattern obtained from electron energy loss spectroscopy of nanocrystalline diamond film [86]

Self-mated reciprocating experiments were performed using a pin-on-flat geometry in Hanks' balanced salt solution (HBSS) and dilute foetal bovine serum (FBS). A nominal contact pressure of 25 MPa was applied for up to 500,000 cycles. Very low friction coefficients of 0.01–0.02 were measured using HBSS, while for FBS lubricated tests the values are slightly higher (0.06–0.09) due to a protein attaching effect. AFM assessed wear rates by an approach using the bearing function for volume loss quantification, yielding wear rates of $k \sim 10^{-10}$ mm^3 N^{-1} m^{-1} in HBSS and $k \sim 10^{-9}$–10^{-8} mm^3 N^{-1} m^{-1} for FBS, characteristic of very mild wear regimes. Similar study was conducted by Amaral et al. [91] using the reciprocating tests under an applied load of 45 N during 500,000 cycles with a NCD-coated Si_3N_4 biocompatible ceramic substrates having two different surface preparations, polished and plasma etched (PE). Friction coefficient values of 0.02

and 0.12 were measured for the polished samples under HBSS and FBS lubrication, respectively. Polished and plasma etched samples showed increased adhesion relative to polished ones and withstood 6 km of sliding distance without any evidence of film fracture but with friction coefficients of 0.06 for HBSS and 0.10 for FBS experiments. Evidences of protein attachment and salt deposition were found, being the responsible for the enhancement of friction under FBS relatively to HBSS. The wear rates measured for the NCD films were in the range of ~10^{-9}–10^{-8} mm^3 N^{-1} m^{-1}, values that are similar to the best values found for ceramic-on-ceramic combinations.

Shenhar et al. [92] employed a simple and original power immersed reaction-assisted coating (PIRAC) nitriding method suitable for surface modification of large complex shape orthopaedic implants of CP Ti and Ti–6Al–4V alloy. CP Ti and Ti–6Al–4V alloy samples were annealed at 1,123–1,373 K in sealed stainless steel containers that allow selective diffusion of nitrogen atoms from the atmosphere. PIRAC-nitrided surfaces were found to have a layered structure with a TiN: Ti_2N coating followed by nitrogen-stabilized α-Ti. In contrast to the coatings obtained by plasma nitriding [93], the compound layer on PIRAC-nitrided Ti–6Al–4V is always thicker than that on CP Ti after similar treatments. In contrast to surface-nitrided Ti–6Al–4V alloy, a Ti_3Al intermetallic phase was detected at the Ti_2N:α–Ti interface acting as a barrier for nitrogen diffusion. Importantly for biomedical applications, no toxic Al or V was detected in the surface layer of PIRAC-nitrided Ti–6Al–4V alloy.

Titania, zirconia, etc., are also considered as bioinert materials. Titanium dioxide (TiO_2) is widely used in biomedical applications because of its excellent biocompatibility. In biomedical implant applications, TiO_2 possesses three major biomedical advantages: corrosion resistance, biocompatibility and blood compatibility. The formation of TiO_2 coatings on Ti–6Al–4V alloys was proposed to ameliorate the biocompatibility of load bearing prostheses [94]. The titania coatings also present a barrier function which would avoid the negative effects of Al and V ions released by wear processes over the Ti–6Al–4V prostheses [95]. Both effects, i.e. apatite nucleation induction and diffusion barrier properties, permit to envisage applications for the improvement of metallic load bearing prostheses, even more when a high bonding strength to the commonly used Ti–6Al–4V alloy is ensured. There are several techniques for preparing titanium dioxide films, such as anodic oxidation [96], thermal oxidation [97], cathodic vacuum arc deposition [98], magnetron sputtering [99], plasma immersion ion implantation (PIII) [100], sol–gel [101], electrosynthesis [102], sol–gel [103], ion beam-enhanced deposition (IBED) [104] and plasma spraying [105]. Plasma-sprayed titanium coatings with porous structure have been used in teeth root, hip, knee and shoulder implants. The porous surface improves fixation via the growth of bone into the coating forming a mechanical interlock. Also TiO_2 thin films fabricated by PIII exhibit superior thromboresistant properties in long-term tests [105].

Zirconium is widely used to build prosthetic devices because of its good mechanical and chemical properties. When exposed to oxygen, zirconium becomes zirconium oxide (ZrO_2) which is biocompatible [106]. Recent studies by Ferranis

et al. [107] and Piconi et al. [108] proved the suitability of zirconia as the best implant material for hard tissue repair due its higher bending strength and fracture toughness. ZrO_2 is a bioinert non-resorbable metal oxide which has been used in dental implants [109] and in femoral heads of total hip replacements. In this case, ZrO_2 ball heads have shown an ultimate compressive load that is 2–2.5 times higher than that of aluminium oxide heads [108]. ZrO_2 is used in prosthetic surgery of the hip giving a prolonged life of the implant because of its low friction surface and low debris products. ZrO_2 implants have an excellent resistance to corrosion and a high wear resistance [110]. ZrO_2 has high affinity for bone tissue [109] and the bone–implant interface is similar to that seen around titanium implants [110]. It was shown that ZrO_2 did not present any signs of toxic, immune or carcinogenetic effects [111] and had no oncogenic effects in vitro [112]. ZrO_2, in fact, is mainly used to enhance bone growth, to minimise friction and corrosion and to improve biocompatibility of total joint prostheses [113]. A good biocompatibility of this material was found in animal studies with direct bone apposition to the implants [114]. ZrO_2 can also be prepared as a colloidal suspension and then used to coat surfaces for improving their characteristics [115]. In another study, Richard et al. [116] investigated the behaviour of new nano ZrO_2 and Al_2O_3-13 wt.% TiO_2 thermal sprayed coatings on commercially pure (CP)-Ti (grade 4) and titanium alloy substrates. Friction and wear tests against Al_2O_3 balls showed that the wear resistance of Al_2O_3-13 wt.% TiO_2 is better than that of ZrO_2 coating. Both plasma sprayings have similar abrasive wear behaviour; however, the average friction coefficient is higher for alumina–titania coating. The major wear mechanism was found to be soft abrasion.

Carbon nitride CN is an excellent candidate for use as biocompatible coatings on biomedical implants [117]. Despite few reports about biocompatibility of CN coating, its novel properties such as extreme hardness and wear resistance [118] are already established. The properties of these coatings are attractive to such medical devices as stents, dental roots, catheters, internal leads and electrodes, guidewires, prostheses, inferior vena cava filters, heart valves, blood tubing, cannulae, dental instrument tips and scalpels. It is also applied as bio-sensors, anti-biofouling coatings for urinary-and blood-based implants, needles, orthopaedic pins, reducing bone cement wear, coatings on artificial heart organs, intraocular lens, etc. [119].

8.3.3 Biotolerant Coating

Diamond-like carbon or DLC coatings are considered to be biotolerant coatings. It is known that DLC shows a low wear and also low friction in atmosphere against most materials except some polymers. DLC has, when sliding against certain materials, the ability to form a transfer layer on the softer counterpart, protecting it from wear. However, it is not clear whether this situation is also present in an in vivo joint where body fluids are capable of reacting with wear products and of

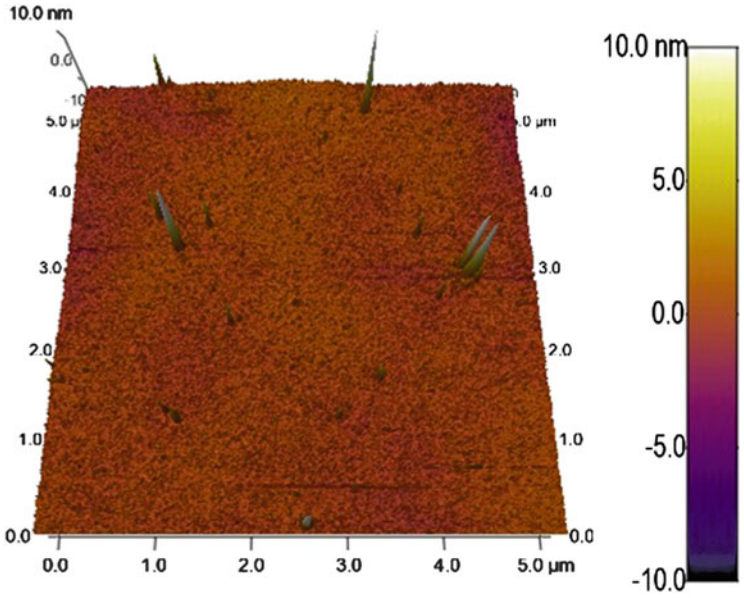

Fig. 8.15 An AFM image showing the topography of ultra smooth carbon film obtained by direct current sputtering

removing wear products out of the tribological contact area. Due to its excellent biocompatibility and good tribological properties, DLC is a promising candidate, as a coating in orthopaedic applications. There are many literatures reporting on experiments using either a ball-on-disc setup or a hip simulator to determine friction and wear of DLC-coated hip joint balls sliding against UHMWPE or of metal/metal joints with one or both sides coated with DLC. Depending on the test setup and especially the liquid lubricant used, different and partially contradicting results can be found in the literature.

DLC films can be deposited with ultra smooth surface finish. Figure 8.15 represents the AFM topography of a DLC film obtained by pulsed direct current sputtering. The roughness parameter for this surface is computed to be 0.6 nm. High amorphicity of the deposited films can also be proven by high resolution transmission electron microscopic investigations. Figure 8.16 shows high resolution transmission electron microscopic (HRTEM) image of DLC film obtained by pulsed direct current sputtering. The non-crystalline nature of deposited films is evident. However, small atomic aggregates in the range of 2–3 nm are found in the DLC matrix.

In order to describe the structure of the diamond-like carbon films with Raman spectroscopy, it is necessary to discuss the intensity ratio I_D/I_G, the full width at half maximum of the G-band (FWHM (G)) and the position of the G-band. First, it has to be considered that the intensity ratio I_D/I_G is a measure of the size of the sp^2 phase organised in rings [120]. If the intensity ratio I_D/I_G becomes lower or zero, the sp^2

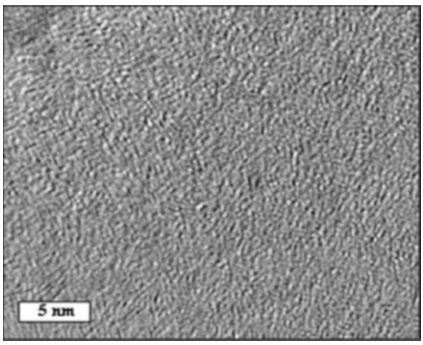

Fig. 8.16 TEM image of ultra smooth carbon film obtained by direct current sputtering

phase is organised rather in chains, whereas a higher intensity ratio I_D/I_G is an indication of an increase of the sp^2 phase in aromatic rings. Thus, if no D-band is visible, no aromatic carbon ring exists in the investigated material [121].

For a-C:H films, where the sp^2 phases and the sp^3 phases are linked together, the visible Raman parameters (532 nm) can be used to reveal information about the sp^3-hybridisated carbon fraction of the films. A lower intensity ratio I_D/I_G is connected with higher overall sp^3 content [122]. Since carbon is sp^3 bonded in a-C:H films also to hydrogen, an increase in sp^3 content does not always mean an increase in density, hardness and other mechanical properties [120, 121]. For a-C:H with hydrogen content over 25 at.% the overall sp^3 content can increase, but not the C–C sp^3 content.

To investigate the structure of the deposited films in more detail it is necessary to focus also on the FWHM (G). The FWHM (G) is a key parameter of monitoring structural disorder in DLC films [117]. This structural disorder arises from the bond angle and bond length distortions in DLC. The FWHM (G) is small when sp^2 clusters are more defect-free and ordered and a higher FWHM (G) is thus indicative for an increase in disorder [120]. The effect originates in the higher bond length and higher bond angle in a more disordered material [120]. The increase in disorder is linked to an increase in C–C sp^3 content, density and hardness [120].

An I_D/I_G ratio of 0.61 $\pm$ 0.03 was calculated with peak amplitudes of the bands shown in Fig. 8.17. Intensities from D and G-bands in spectra taken from samples deposited at higher C_2H_2/Ar-ratios of 0.11–0.25 at similar process parameters show relatively constant I_D/I_G ratios of 0.62 $\pm$ 0.04 and 0.64 $\pm$ 0.01, respectively. Therefore the size of graphitic clusters is not much influenced in this process window. Sputtering at the highest used C_2H_2/Ar-ratio of 0.43 resulted in a film structure with an I_D/I_G ratio of 0.55 $\pm$ 0.05. From these data, the trend of a decreased clustering of sp^2 phases in aromatic rings in the film deposited with the highest C_2H_2/Ar-ratio can be deduced [120, 121, 123, 124].

The position of the G-band moved down from 1,550 $\pm$ 4 cm^{-1} (C_2H_2/Ar-ratio of 0) to 1,546 $\pm$ 1 cm^{-1} (C_2H_2/Ar-ratio of 0.43). The lower I_D/I_G ratio for this film is evident for a higher overall sp^3 binding content [120, 121, 123, 124]. Here it has to be considered, that in a-C:H the carbon atom can form bonds to carbon as

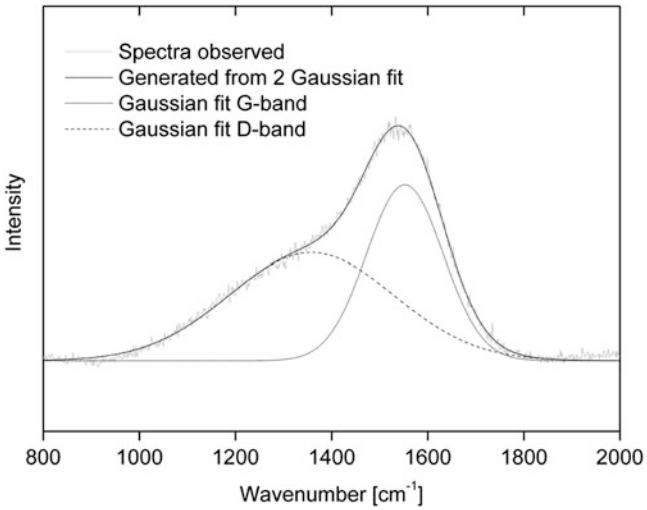

Fig. 8.17 A typical Raman spectra obtained from ultra smooth carbon film obtained by direct current sputtering

well as to hydrogen. Therefore it is difficult to identify variances in C–C and C–H bonds in a-C:H films by using the I_D/I_G ratio only. In order to investigate the trends in the C–C sp^3 binding content, the FWHM (G) is used to reveal information about the structural variance induced by changes in the C_2H_2/Ar-rate. It is found, that to the increase of the C_2H_2/Ar-rate shows a decreased structural disorder verified by the decreased FWHM (G) from 191 ± 3 cm^{-1} to 173 ± 1 cm^{-1} (Fig. 8.17). The decrease in disorder can here be linked to a decrease in C–C sp^3 content in the films [120]. Additionally, the film deposited with the highest used C_2H_2/Ar-ratio of 0.43 has the highest C–H sp^3 binding content in the investigated film series.

Evolution of the background slopes arising in the spectra showed unaffected backgrounds with no increasing photoluminescence caused by elevated hydrogen contents in DLC films when using a relatively high excitation wavelength of 532 nm in Raman spectroscopy. The Raman spectra indicate a hydrogen content of roughly ≤25 at.%, which could be estimated from the ratio of the fitted background slope (m) per intensity of the G-band (I_G) [121] of ~0 μm.

Biotribology of DLC films is studied extensively. Hydrogen-free DLC, also named ta-C, coated metal hip joint balls tested in 1 wt.% NaCl water by ball-on-disc and in a hip joint simulator showed a reduced wear of the UHMWPE cup by a factor of 10–100, compared to the uncoated samples [125, 126]. Additionally, an increase in the corrosion resistance of the metallic material was obtained by the coating [126]. A decrease of a factor of five in wear of the UHMWPE was obtained by coating the cobalt chromium counterface with DLC when tested in a knee wear simulator using distilled water as a lubricant [127]. Different coatings have been tested with a ball-on-disc, also using distilled water as a lubricant, and a large decrease in UHMWPE wear was obtained with all the coatings. However, the

thermally oxidised Ti–6Al–4V surface still performed about eight times better than the DLC coating [128]. Analogously, DLC-coated stainless steel femoral heads have been tested against UHMWPE cups in a hip joint simulator using distilled water as a lubricant. A decrease of the UHMWPE wear by a factor of six was obtained due to the DLC coating. The same low wear of the UHMWPE was also obtained when using a zirconia femoral head under the same test conditions [129]. Sheeja et al. [130] prepared multilayer ta-C films by the filtered cathodic arc method from pure C targets. The wear tests of the CoCrMo/UHMWPE and DLC/UHMWPE sliding pairs have been made in water and simulated body fluid on a ball-on-disc apparatus and, in contradiction to the results presented above, no significant difference in wear could be measured between the coated and the uncoated samples [131]. Saikko et al. [132] compared the wear of UHMWPE cups operated against CoCr, alumina and DLC-coated CoCr hip joint balls in a biaxial hip wear simulator in the presence of diluted calf serum. For all three combinations tested, they obtained wear rates of the UHMWPE cups between 48 and 57 mg per one million cycles. There was no significant difference in the wear due to the DLC coating and all wear values obtained were in the range known from clinical observations with CoCr and alumina hip joint balls. Similar results have been obtained also by Affatato et al. [133]. Femoral heads made from 316L stainless steel, alumina, CoCrMo and DLC-coated TiAlV have been tested in a hip joint simulator using bovine calf serum as a lubricant. They obtained wear rates of the UHMWPE cups between 25 and 37 mg per million cycles for all four material combinations tested. From the results shown above, it can be seen that apparently contradicting results on the wear of DLC-coated joints sliding against UHMWPE are obtained. There are several issues presented below which may explain these differences found in the literature. The experimental setup and especially the liquid lubricant used in a tribological test are found to have a crucial influence on the friction and wear values obtained as well as on the type of wear particles produced [134–136]. It was suggested that when bovine serum or synovial fluid was used as a lubricant, the different proteins, especially phospholipids, adsorbed on the surfaces, strongly influences the tribological behaviour in the joints [136] and that also when the protein concentration is too low. The results may show a non-clinically relevant wear morphology [135]. Further, the surface texture has a decisive influence on the wear behaviour of a joint. Even single scratch, which may not be detected by an average surface roughness measurement, is capable of increasing the wear rate of UHMWPE by a factor of 30–70 [137]. Depending on the coating and the tribological conditions, DLC is able to form a transfer layer on the counterpart even in distilled water [138]. However, no transfer layer is formed in biological media against UHMWPE and the UHMWPE still shows wear. To summarise, it should be stated that wear tests on load-bearing implants having a polymer as a counterpart should be made in an appropriate tribological setup such as an implant joint simulator. As a lubricant, a supply of a solution containing an adequate distribution of proteins has to be maintained to compensate for the proteins decomposed in the test due to high pressures between contact spots of

the bearing. Additionally, the surface texture of the areas involved in the tribological process must be characterised carefully.

Platon et al. [139] compared the friction and wear on different material couples used for hip prostheses. Contact pressure was found to be the main parameter which governs wear of materials especially for UHMWPE. The contact pressure in ball-on-disc tests can be controlled in the whole range by the value of ball radius. Results obtained with several different tested materials (stainless steel/UHMWPE, stainless steel + DLC coating/UHMWPE, stainless steel + DLC coating/stainless steel + DLC coating, titanium alloy + DLC coating/UHMWPE, titanium alloy + DLC coating/titanium alloy + DLC coating, zirconium dioxide/UHMWPE, alumina/UHMWPE, alumina/alumina) have shown the superiority of DLC coatings. Dry friction of DLC coatings, in comparison with UHMWPE, leads to a very low wear rate, approximately equal to an alumina couple. Thus, the use of metallic heads with DLC coating in hip prostheses can avoid ruptures observed with ceramic materials at the head–neck joint.

In a study due to Shi et al. [140], the tribological performances of several candidate implant materials, including the diamond-like carbon (DLC) thin film coating on stainless steel were investigated. A pin-on-flat contact configuration in reciprocating sliding was used for preliminary materials evaluation and friction and wear testing. Test pairs were lubricated with bovine blood serum. The DLC coating sliding against uncoated stainless steel showed the lowest friction coefficient and very little, if any, wear as shown in Fig. 8.18. Wear mechanisms in tests of ceramics and steel pairs were primarily abrasive. Similarly Kim et al. [141] reported improved performance of DLC-coated Ti-based dental abutment screw.

In the case of a metal/metal joint with both sides coated with DLC, very low wear rates have been reported. Lappalainen et al. [142], Tiainen [125] investigated hip joints with both sides having a 100-μm thick layer of hydrogen-free DLC made by filtered pulsed plasma arc discharge (85 % sp^3 bonding). Using a hip joint simulator and aqueous NaCl as a lubricant, a reduction of the wear rates, by a factor of about 10,000, corresponding to wear rates of 10^{-3}–10^{-4} mm^3 $year^{-1}$, has been reported [125]. The long duration wear tests of 15 million cycles (corresponding to about 15 years of use) performed by Lappalainen et al. with a hip joint simulator and using bovine serum as a lubricant, which was replaced regularly to compensate for depleted proteins, showed extremely low wear below 10^{-4} mm^3 $year^{-1}$ [142]. Shi et al. [140] tested steel, ceramic and a 2-μm thick DLC (a-C:H)-coated steel ball all sliding against a flat steel plate and using bovine serum as lubricant. They found a severe reduction of the ball wear by about a factor of 100 as well as reduced wear rate in the stainless steel plate. The situation of DLC sliding against DLC may be different than DLC sliding against UHMWPE. The test performed in aqueous NaCl did lead to very low wear values, comparable to those obtained in bovine serum, indicating that a similar wear mechanism takes place in both cases. The build up of a transfer layer may not be a key requirement for low wear (analogous to DLC/sapphire in atmosphere [143]) or may not be severely altered by the presence of proteins.

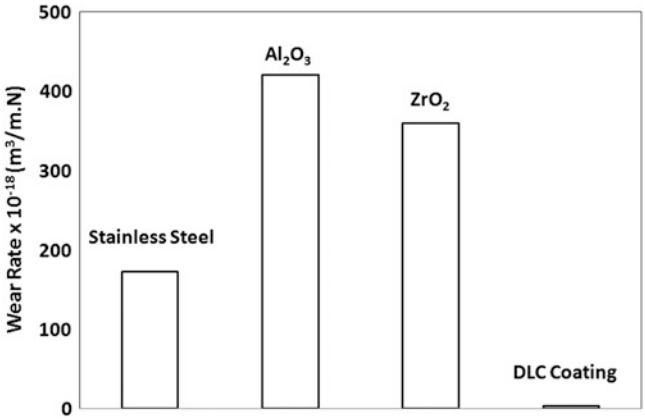

Fig. 8.18 Bar diagram showing the wear rate of Al_2O_3, ZrO_2 and DLC coating sliding against uncoated stainless steel [140]

French company 'Matériels Implants du Limousin SA (M.I.L. SA)' commercially offered DLC-coated titanium shoulder joint balls and ankle-joints with both parts (the tibial and the talar component) made from a nitrided AISI Z5 CNMD 21 steel and coated with DLC. In 2001, the company 'Implant Design AG' sold knee joints under the trade name 'Diamond Rota Gliding' with the sliding area of the femur component coated with DL N (diamond-like nanocomposite, a SiO_x containing DLC described in [144]) which was sliding against UHMWPE. Recently Teager et al. [145] published data about the clinical failure rate of a 8-year follow-up on 101 patients with implanted DLC-coated femoral balls articulating against polyethylene. The DLC-coated femoral heads with the trade name Adamante had been obtained from Biomecanique, France. They consisted of a 2–3-μm thick DLC coating on a Ti–6Al–4V alloy ball, made by ion-beam deposition. Whereas the DLC-coated implants showed no sign of problems within the first 1.5 years. Subsequently, more and more DLC implants showed aseptic loosening requiring revision (replacement) of the implant. The currently accepted explanation for aseptic loosening is that wear debris generated from the prosthesis initiates a macrophage-mediated inflammatory response, leading to osteoclast cells activation resulting in bone resorption. Within 8.5 years, 45 % of the originally implanted DLC-coated joints had to be replaced. The DLC coating on the retrieved joint heads showed numerous mostly round shaped pits. When a coating is deposited onto a metallic substrate, usually about 1 nm thick reaction layer is formed at the interface and this layer is responsible for good adhesion. Depending on the precleaning and the conditions at the very beginning of the DLC deposition process, the interface reaction layer consists usually of a metal-carbide or metalhydro-oxy-carbide. The long-term chemical stability of this reaction layer has to be guaranteed also under in vivo conditions. That biological fluids, particularly phosphate buffered saline solution (PBS), can penetrate the coating through pinholes and slowly corrode the interface between DLC and a-Si:H/DLC is described in [146]. An example of a

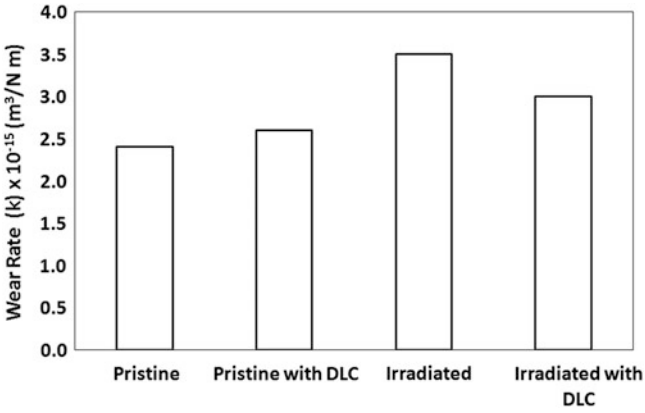

Fig. 8.19 The bar diagram showing the improved wear rate of DLC-coated UHMWPE than uncoated UHMWPE [148]

chemical instable interface leading to ongoing delamination even during storage in ambient atmosphere is given in [147]. Interface delamination due to interface corrosion involves also residual stress and electrochemical aspects and is not fully understood today.

Puértolas et al. [148] deposited hydrogenated diamond-like carbon (DLCH) thin films on medical grade ultra high molecular weight polyethylene (UHMWPE) by radio frequency plasma-enhanced chemical vapour deposition. The substrates were discs made of UHMWPEs typically used for soft components in artificial joints, namely virgin GUR 1050 and highly crosslinked (gamma irradiated in air to 100 kGy) UHMWPEs. Tribological properties under bovine serum lubrication at body temperature were assessed on coated and uncoated polyethylenes by means ball-on-disc tests. Morphological features of the worn surfaces were obtained by confocal microscopy and scanning electron microscopy. The wear factors k of the coated and uncoated surfaces were determined according to the following equation.

$$k = \frac{2\pi r A_m}{Ls} \tag{8.1}$$

where r is the wear track radius, A_m is the average worn area, L is the applied load and s is the sliding distance. The result of their observation is given in Fig. 8.19 in the form of bar diagram. This study confirms an increase in wear resistance for coated materials after 4,400 m of sliding test compared to uncoated polyethylene. These results point out that UHMWPE coated with DLCH films could be a potential method to reduce backside wear in total hip and knee arthroplasties.

Varieties of metal containing nanocomposite DLCs such as Ti alloyed, Cr alloyed and Si alloyed are developed [149–152] and these films have promising future in biomedical application. In general, these nanocomposite films exhibit better response to cell seeding than amorphous carbon films. The seeding behaviour

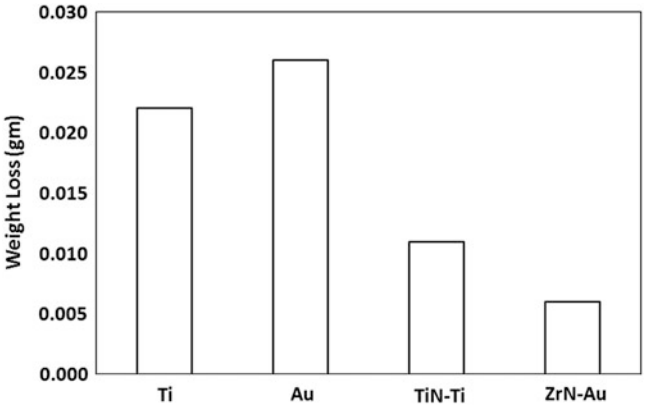

Fig. 8.20 Bar diagram showing the weight loss of TiN and ZrN coating ion plated on abutment screw made of Ti and gold respectively [153]

of endothelial cell on diamond-like carbon surface is governed by contact angle, surface energy, resistivity, work function, contact potential difference and atomic dopant concentration. Consequently these coatings have potential applications not only in prosthetic joints but also in cardiovascular devices such as heart valves, etc.

Another important biotolerant coating is TiN. Choe et al. [153] found improved wear performance of TiN ion-plated Ti dental screw and ZrN ion-plated dental gold screw as shown in Fig. 8.20. Similar observation for abutment screw was also made by Jung et al. [154]. Gispert et al. [155] attempted to improve the tribological behaviour of the prosthetic pair TiN-coated stainless steel/ultra high molecular weight polyethylene (UHMWPE) by chlorine implantation of the TiN surface. Friction and wear were determined using a pin-on-disc apparatus and the wear mechanisms were investigated through scanning electron microscopy (SEM) and atomic force microscopy (AFM). Chlorine implantation led to a significant polymeric wear reduction when the lubricant was Hanks' balanced salt solution (HBSS). If bovine serum albumin (BSA) was added to HBSS, a strong decrease of both friction and polymeric wear was observed for implanted and non-implanted TiN coatings. The former case was explained by the formation of a titanium oxide layer on the TiN surface, while the latter derived from albumin adsorption. Wear reduction may be attributed to the substitution of the hard TiN counterface by a titanium oxide layer with lower hardness which is a less wear aggressive for the polymer surface. The behaviour of the friction coefficient was attributed to the slow precipitation of calcium phosphate. When albumin was added to HBSS, friction and wear decreased significantly due to protein adsorption but still, the Cl-implanted TiN coating led to the best tribological results.

Wang et al. [156] studied the tribological properties of TiN and DLC coatings in a simulated body fluid (SBF) environment. The ball-on-plate impact tests were conducted on the coatings under a combined force of a 700 N static load and a 700 N dynamic impact load for 10,000 impacting cycles. The results indicated that

the TiN and DLC coatings exhibited an excellent wear resistance and chemical stability during the sliding tests against a high density polyethylene (HDPE) biomaterial. Compared to the DLC coating, the TiN coating has a better compatibility with the HDPE. However, the impact tests showed that the fatigue cracks and the coating chipping occurred on the TiN coating but not on the DLC coating. In a separate study, the performance of three titanium nitride coatings: TiN, TiNbN and TiCN for biomedical applications were assessed in terms of their surface properties, cytotoxicity and tribological performances by Serro et al. [157]. The tribological behaviour of the coatings rubbing against UHMWPE in lubricated conditions was investigated using a pin-on-disc apparatus. Albumin adsorption on the three coatings was studied with a quartz crystal microbalance with dissipation (QCM-D) and AFM scratching. Cytotoxicity was determined both in direct or indirect contact of the cells with the coating materials. The results demonstrate that the three coatings have similar surface properties and are not cytotoxic. TiNbN showed the best tribological performance in the presence of albumin, although albumin adsorption was slightly higher on TiN. Friction and wear of polyethylene counterfaces against the three coatings were found to depend on the lubricant in HBSS. TiN was the best solution while TiNbN seemed to be a better choice when albumin was added to HBSS.

A modified pin-on-disc machine was used by Hoseini et al. [158] for the tribological investigation of ultrahigh molecular weight polyethylene (UHMWPE) sliding on stainless steel or stainless steel coated with diamond-like carbon, titanium nitride or 'Micronite'. 'Micronite' is a new type of coating applied by a physical vapour deposition technique combined with a very low friction coating material giving improved tribological properties. The tribological parameters used were chosen to mimic the conditions prevailing in the human body. The wear debris and the counter-surfaces were analysed. The surface analysis showed that the coating changed the roughness of the counter-surfaces. The diamond-like carbon and 'Micronite' coatings had a much higher surface roughness than the titanium nitride coating. The results shown in Fig. 8.21 indicated that the enhanced tribological behaviour of the 'Micronite'/UHMWPE sliding pair justified their usage as a material combination in artificial joints. Figure 8.21 essentially indicates friction coefficient and specific wear of UHMWPE against various coatings.

Tribological screening tests (simple, reciprocating ball-on-flat tests) were performed with the objective to identify an appropriate coating for the articulating surfaces of artificial hip joints whose acetabular cups and femoral stems are made from Ti–6Al–4V alloy by Osterle et al. [159]. Their results are presented in Fig. 8.22. Standard coatings like TiN or CrN performed better than more complicated multi-layer systems. These coatings, however, did not perform as good as different types of amorphous carbon coatings, generally referred to as diamond-like carbon or DLC coatings. Among the DLC coatings, hydrogenated amorphous carbon (a-C:H) displayed the best properties, especially if the hydrogen content was increased by reducing the bias voltage during PA-CVD-deposition. The optimised a-C:H coating revealed the most promising wear behaviour under the applied testing conditions [149]. Aluminised and chromised high carbon steel also exhibited promising performances in physiological solution [160]. Regarding the

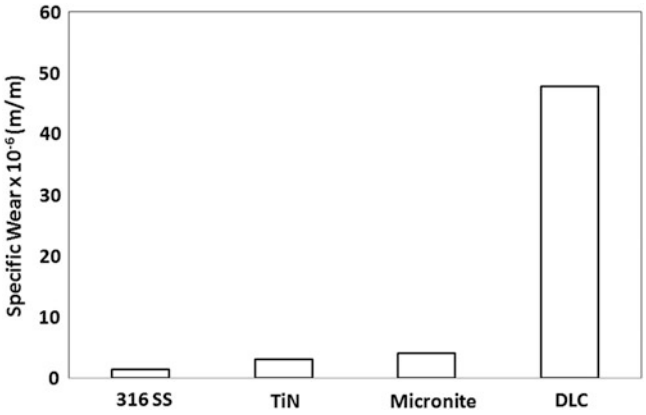

Fig. 8.21 Bar diagram indicating the enhanced tribological behaviour of the Micronite/UHMWPE sliding pair used as a material combination in artificial joints [158]

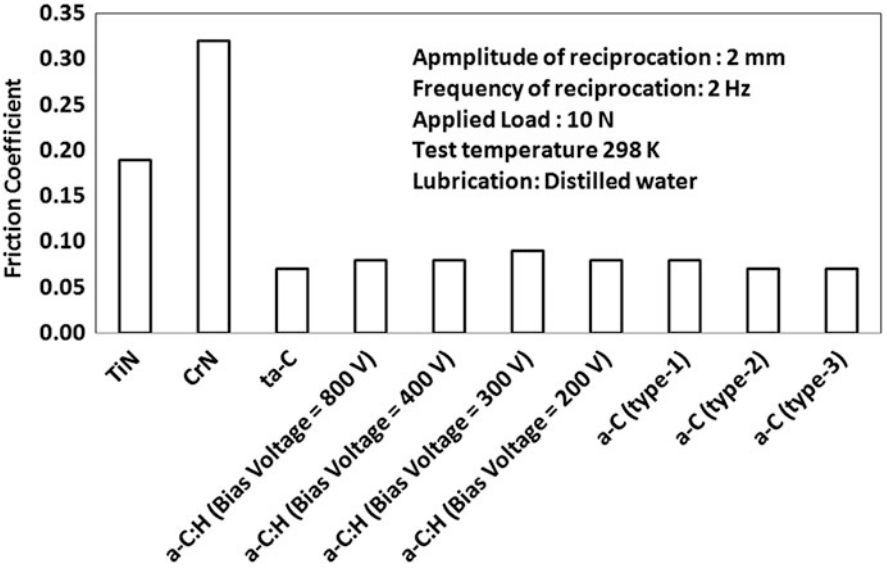

Fig. 8.22 Bar diagram showing the friction behaviour of various coatings primarily DLC films [159]

materials examined, correlation of wear with mechanical properties obtained by nano-indentation revealed that high hardness was not an adequate criterion for selecting appropriate coatings. A high ratio of hardness and elastic modulus (H/E) proved to be more important [161]. Microstructural and micro-analytical investigations revealed transformation of TiN and CrN to TiO_2 and Cr_2O_3, respectively, and amorphous carbon was, at least partly, transformed to graphite. Furthermore, incorporation of Al_2O_3 from the ball was observed at a very fine scale. The wear

debris of favourable coatings always formed agglomerates of nanoscale particles. It was shown that commercial nano-particles of Al_2O_3, Cr_2O_3 and carbon black are comparable to particles generated by the tribological tests. However, it is uncertain whether they are comparable to those formed during simulator studies or in vivo.

Unsworth [162] defined a parameter similar to friction coefficient and known as friction factor given as

$$f = \frac{T}{rL} \tag{8.2}$$

Where T is the torque, r is the radius of the femoral head and L is the applied load. With the help of a hip simulator, the friction factor and film thickness was calculated [126] for metal/metal, metal/ceramic and metal/polymer hip joint lubricated with bovine serum or aqueous solution of carboxyl methyl cellulose. Calculated film thickness varied from 0.05 to 0.09 μm.

8.4 Summary and Outlook

Thus a variety of coatings and surface modification techniques have been identified as potential methods for improved performances of large variety of tribological issues of human body. Even modification of amorphous diamond-like carbon coatings with addition of metals such as Si, Cr results in formation of nanocomposite coatings with better biocompatibility. A successful exploitation of these devices is the main aim of scientific research and clinical application. Success of such application depends on surgery process, size and design of implants, their anatomical location, biological environment and age and sex of the patients. Laser-assisted direct metal deposition technique also offers huge potential as future manufacturing technologies for orthopaedic implants. Since this method is based on the concept of three-dimensional stereolithography and is capable of restructuring a 3D shape using computer in a short time, this technology can be adopted to manufacture custom design implant. DLC and TiN coatings can be considered to be potential areas of application in artificial heart valves, bearings of heart pump, left ventricular assist device, catheters, etc.

Biometric approach appears to offer new horizon in clinical research for tribology-related application. This method allows desired coating with bone-like homogenous composition. Nanoapetite coatings can also be deposited by this method. The next stage of development in orthopaedic and dental field is biomimetic bone implant. Biomimetic implants are not available commercially at this moment as the possibility of undesirable bone tissue reaction is still not eliminated. The combination of biomimetic nanoapatite and bone implants may result in a nanophase osteogenesis on orthopaedic and dental implant. Various nanomimetic materials investigated so far include ceramics, metals, polymers, composites and carbon nanofibre and nanotubes. The hybrid coatings with nanophase biomaterials

provide a new method to design implant surfaces for next generation prostheses. The unique nanoporous microstructural properties of nanomaterials allow strong selective adsorption of molecular architectures making hybrid coating a potential carrier for therapeutic agents [163, 164]. It is possible to enhance the regeneration and healing of bone and soft tissues by nanoscale modification of bone implant surfaces by incorporating biological agents into nanostructure materials.

The usage of traditional coarse-grained plasma-sprayed HA coatings on joint replacements and dental implants will be replaced by nanostructured CaP coatings. Nano-porous HA-coated drug-eluting stents will partly replace the current polymer-coated drug-eluting stents. Owing to high biocompatibility of HA nanocrystals for microvascular endothelium [165], such stents will be less thrombogenic and will probably require only short-term anticoagulant therapy [166]. New future directions are aimed at creating therapeutic coatings that have a dual beneficial effect namely osteoconductive properties combined with the ability to deliver therapeutic agents, proteins and growth factors directly into the coating. These new coatings may offer the ability to stimulate bone growth, combat infection, and ultimately, increase implant lifetime [167]. A different route in the quest for new promising biomaterials is based on ceramic–polymer composites that are being designed to mimic the mechanical and biological performance of natural bone. Such novel materials have been designed 'intelligent' and are defined as human-friendly materials that can change their characteristics in response to surrounding conditions, for example, varying stress fields [168]. Tribological studies of all these new coatings in physiological solution will certainly give new dimension on joint replacement or other implants of human body.

The combination of bioactivity and biodegradability is probably the most relevant characteristics of the next generation of the biomaterials. These properties should merge with the ability to signal and stimulate specific cellular activity and behaviour. Biodegradable composite scaffolds, unresorbable porous metallic and polymer foams can be considered as perspective materials. Their surface bioactivation can be achieved by functionalizing surfaces with different biomolecules by applying a variety of methods where both chemical bonding and physical adsorption take place. Some more sophisticated 'bottom-up' and 'top-down' techniques should be developed to engineer surfaces with high specificity levels. The task of tailoring the biomaterials' surfaces for at least some of the different purposes of implant integration and tissue regeneration seems a feasible challenge in the future, probably at midterm by the synergistic interdisciplinary work of materials science, engineering, biology, chemistry, physics and medicine.

References

1. Gawaz M, Neumann FJ, Ott I, May A, Schomig A (1996) Circulation 94:279
2. Lahann J, Klee D, Thelen H, Bienert H, Vorwerk D, Hocker H (1999) J Mater Sci Mater Med 10:443

3. Bittl J (1996) N Engl J Med 335:1290
4. Haycox CL, Ratner BD (1993) J Biomed Mater Res 27:1181
5. Yang Y, Franzen SF, Olin CL (1996) J Heart Valve Dis 5:532
6. Dowson D (1995) Wear 190:171
7. Podsiadlo P, Stachowiak GW (1999) Wear 230:184
8. Campbel AA (2003) Mater Today 11:26
9. Barril S, Mischler S, Landolt D (2005) Wear 259:282
10. Windler M, Klabunde R, Brunette DM et al (eds) (2001) Titanium in medicine. Springer, Berlin, p 703
11. Hallab NJ, Jacobs JJ (2003) Corros Rev 21:183
12. Hiromoto S, Mischler S (2006) Wear 261:1002
13. Dobies DR, Cohoon A (2006) J Invasive Cardiol 18(5):E146–E148
14. Daculsi G (1998) Biomaterials 19:1473
15. Ducheyne P, Qiu Q (1999) Biomaterials 20:2287
16. Busur D, Ruskin J, Higginbottom F, Hartdwick R, Dahlin CC, Schenk R (1995) Intl J Oral Maxillofac Implants 10:666
17. Ong JL, Carnes DL, Bessho K (2004) Biomaterials 25:4601
18. Loty C, Sautier JM, Boulekbache H, Kokubo T, Kim HM, Forest N (2000) J Biomed Mater Res 49:423
19. Kokubo T, Kim HM, Kawashita M (2003) Biomaterials 24:2161
20. Li P, Kangasniemi I, De Groot K (1993) Bioceramics 6:41
21. Piconi C, Maccauro G (1999) Biomaterials 20:20
22. Adolfsson E, Hermanson L (1999) Biomaterials 20:1263
23. Kola PV, Daniels S, Cameron DC, Hashmi MSJ (1996) J Mater Process Technol 56(1–4):422
24. Knotek O, Loffler F, Weitkamp K (1992) Surf Coat Technol 55(1–3):536
25. Dion I, Roques X, More N (1993) Biomaterials 14:712
26. Van Raay JJAM, Rozing PM, Van Blitterswijk CA, Van Haastert RM, Koerten HK (1995) J Mater Sci Med 6:80
27. Huang N, Yang P, Leng YX, Chen JY, Sun H, Wang J, Wang GJ, Ding PD, Xi TF, Leng Y (2003) Biomaterials 24:2177
28. Li P, Ohtsuki C, Kokubo T, Nakanishi K, Soga N, de Groot K (1994) J Biomed Mater Res 28:7
29. Hench LL, Spinter RJ, Allen WC, Greenlee TK Jr (1971) J Biomed Mater Res 2(1):117
30. De Groot K (1991) Centennial Mem Issue 99(10):943
31. Bolz A, Schaldach M (1990) Artif Organs 14:260–269
32. Shtansky DV, Gloushankovab NA, Sheveiko AN, Kharitonova MA, Moizhess TG, Levashov EA, Rossi F (2005) Biomaterials 26:2909
33. Shtansky DV, Gloushankova NA, Bashkova IA, Petrzhik MI, Sheveiko AN, Kiryukhantsev-Korneev FV, Reshetov IV, Grigoryan AS, Levashov EA (2006) Surf Coat Technol 201:4111
34. Shtansky DV, Levashov EA, Glushankova NA, D'yakonova NB, Kulinich SA, Petrzhik MI, Kiryukhantsev-Korneev FV, Rossi F (2004) Surf Coat Technol 182:101
35. Shtansky DV, Gloushankova NA, Bashkova IA, Kharitonova MA, Moizhess TG, Sheveiko AN, Kiryukhantsev-Korneev FV, Osaka A, Mavrin BN, Levashov EA (2008) Surf Coat Technol 202:3615–3624
36. Shtansky DV, Gloushankova NA, Sheveiko AN, Kiryukhantsev-Korneev PV, Bashkova IA, Mavrin BN, Ignatov SG, Filippovich SY, Rojas C (2010) Surf Coat Technol 205:728–739
37. Leyland A, Matthews A (2000) Wear 246:1
38. Shtansky DV, Grigoryan AS, Toporkova AK, Sheveiko AN, Kiruykhantsev-Korneev PV (2011) Surf Coat Technol 206:1188–1195
39. Shtansky DV, Gloushankova NA, Bashkova IA, Kharitonova MA, Moizhess TG, Sheveiko AN, Kiryukhantsev-Korneev FV, Petrzhik MI, Levashov EA (2006) Biomaterials 27:3519
40. Park JH, Lee YK, Kim KM, Kim KN (2005) Surf Coat Technol 195:252
41. Kokubo T (1985) J Mater Sci 20:2001

42. Holmes RE (1986) J Bone Joint Surg Am 68:904
43. Bucholz RW et al (1989) Clin Orthop 240:53
44. Osborne JF, Newesley H (1980) In: Heimke G (ed) Dental implants. Carl Hansen, Munich
45. Orly I et al (1989) Calcif Tissue Int 45:45
46. Ducheyne P (1987) J Biomed Mater Res 21(A2):219
47. Fujiu T, Ogion M (1984) J Biomed Mater Res 18(7):845
48. Daculsi G et al (1989) J Biomed Mater Res 23:849
49. Tracy BM, Doremus RH (1984) J Biomed Mater Res 18:719
50. Hench LL (1998) J Am Ceram Soc 81:1705
51. Wen J et al (2000) Biomaterials 21:1339
52. Dong ZL et al (2003) Biomaterials 24:97
53. Zhang C et al (2001) Biomaterials 22:1357
54. Thomas MB et al (1980) J Mater Sci 15:891
55. de With G et al (1981) Mater Sci 16:1592
56. Buser D et al (1991) J Biomed Mater Res 25:889
57. Jansen JA et al (1991) J Biomed Mater Res 25:973
58. Soballe K et al (1990) Acta Orthop Scand 61(4):299
59. Choi WJ et al (1998) J Am Ceram Soc 81:1743
60. Kong YM et al (1999) J Am Ceram Soc 82:2963
61. Lemons JE (1988) Clin Orthop 235:220
62. Kyeck S, Remer P (1999) Mater Sci Forum 308–311:308
63. Ong JL et al (1991) J Am Ceram Soc 74:2301
64. Dasarathy H et al (1996) J Biomed Mater Res 31:81
65. Yamashita K et al (1996) J Am Ceram Soc 79:3313
66. Hero H et al (1994) J Biomed Mater Res 28:343
67. de Bruijn JD et al (1992) J Biomed Mater Res 26:1365
68. Hench LL, Paschall HA (1973) J Biomed Mater Res Symp 7(3):25
69. Ban S et al (1994) J Biomed Mater Res 28:65
70. Guipont V, Espanol M, Borit F, Llorca-Isern N, Jeandin M, Khor KA, Cheang P (2002) Mater Sci Eng A 325:9
71. Chang E, Chang WJ, Wang C, Yang CY (1997) J Mater Sci Mater Med 8:193
72. Gaona M, Fernandez J, Guilemany JM (2006) In: Proceedings of international thermal spray conference, 15–17 May, Seattle, WA
73. Ning CY, Wang YJ, Lu WW, Qiu QX, Lam RWM, Chen XF, Chiu KY, Ye JD, Wu G, Wu ZH, Chow SP (2006) J Mater Sci Mater Med 17:875
74. Lamy D et al (1996) J Mater Res 11:680
75. Liu X, Ding C (2002) Biomaterials 23:4065
76. Fu Y, Batchelor AW, Khor KA (1999) Wear 230:98
77. Diomidis N, Mischler S, More NS, Roy M (2012) Acta Biomater 8:852
78. More N, Diomidis N, Paul SN, Roy M, Mischler S (2011) Mater Sci Eng C 31:400
79. Sahu S, Palaniappa M, Paul SN, Roy M (2010) Mater Lett 64:12
80. Keicher DM, Smugeresky JE (1997) J Met 49(5):51
81. Griffith M, Schlienger ME, Harwell LD, Oliver MS, Baldwin MD, Ensz MT, Esien M, Brooks J, Robino CE, Smugeresky JE, Hofmeister W, Wert MJ, Nelson DV (1999) Mater Des 20(2–3):107
82. Long M, Rack HJ (2005) Mater Sci Eng C 25(3):382
83. Long M, Rack HJ (2001) Wear 249:158
84. Samuel S, Nag S, Scharf T, Banerjee R (2007) Mater Sci Eng C 28(3):414
85. Erdemir A, Fenske GR, Krauss AR, Gruen DM, McCauley T, Csencsits RT (1999) Surf Coat Technol 120–121:565
86. Roy M, Steinmuller-Nethl D, Tomala A, Tomastik C, Koch T, Pauschitz A (2011) Diam Relat Mater 20:573
87. Papo MJ, Catledge SA, Vohra YK (2004) J Mater Sci Mater Med 15:773

88. Fries MD, Vohra YK (2002) J Phys D Appl Phys 35:L105
89. Met C, Vandenbulcke L, Sainte Catherine MC (2003) Wear 255:1022
90. Amaral M, Abreu CS, Oliveira FJ, Gomes JR, Silva RF (2007) Diam Relat Mater 16:790
91. Amaral M, Abreu CS, Oliveira FJ, Gomes JR, Silva RF (2008) Diam Relat Mater 17:848
92. Shenhar A, Gotman I, Gutmanas EY, Ducheyne P (1999) Mater Sci Eng A268:40
93. Rie K-T, Lampe TH (1985) Mater Sci Eng 69:473
94. Manso M et al (2002) Biomaterials 23:349
95. Long M, Rack HJ (1998) Biomaterials 19:1621
96. Pouilleau J, Devillers D, Garrido F, Durand-Vidal S, Mahe E (1997) Mater Sci Eng B 47:235
97. Lin C-M, Yen S-K (2004) J Electrochem Soc 151(12):D127–D133
98. Bendavid A, Martin PJ, Takikawa Thin H (2000) Solid Films 360:241
99. Amor SB, Baud G, Besse JP, Jacquet M (1997) Mater Sci Eng B 47:110
100. Mandl S, Thorwarth G, Schreck M, Stritzker B, Rauschenbach B (2000) Surf Coat Technol 125:84
101. Liqiang J, Xiaojum S, Weimin C, Zili X, Yaoguo D, Honggang F (2003) J Phys Chem Solids 64:615
102. Natarajan C, Nogami G (1996) J Electrochem Soc 143:1547
103. Li P, Kangasniemi I, De Groo K (1993) Bioceramics 6:41
104. Huang N, Yang P, Chen X (1998) Biomaterials 19:771
105. Liu X, Chu PK, Ding C (2004) Mater Sci Eng R47:49
106. Carinci F, Pezzetti F, Volinia S, Francioso F, Arcelli D, Farina E (2004) Biomaterials 25 (2):215
107. Ferraris M, Verné E, Appendino P, Moisescu C, Krajewski A, Ravaglioli A, Piancastelli A (2000) Biomaterials 21:765
108. Piconi C, Maccauro G (1999) Biomaterials 20(1):1–25
109. Akagawa Y, Ichikawa Y, Nikai H, Tsuru H (1993) J Prosthet Dent 69:599–604
110. Rosengren A, Pavlovic E, Oscarsson S, Krajewski A, Ravaglioli A, Pincastelli A (2002) Biomaterials 23(4):1237
111. Hulbert SF, Morrison SJ, Klavitter JJ, Biomed J (1972) Mater Res 6:347–374
112. Covacci V, Bruzzese N, Maccauro G, Andreassi C, Ricci GA, Piconi C (1999) Biomaterials 20(4):371–376
113. Kim BK, Bae HE, Shim JS, Lee KW (2005) J Prosthet Dent 4:357
114. Akagawa Y, Hosokawa R, Sato Y, Kameyama K (1998) J Prosthet Dent 80:551–558
115. Lappalainen R, Anttila A, Heinonen H (1998) Clin Orthop Relat Res 352:118–127
116. Kokubo T (1990) J Non Cryst Solids 120:138
117. Cui FZ, Li DJ (2000) Surf Coat Technol 131:481–487
118. Quiros C, Nunez R, Priet P et al (1999) Vacuum 52:199
119. Mcaughlin JA, Maguire PD (2008) Diam Relat Mater 17:873
120. Casiraghi C, Ferrari AC, Robertson J (2005) Phys Rev B 72:085401
121. Ferrari AC, Robertson J (2004) Philos Trans R Soc Lond A 362:2477
122. Ronkainen H, Koskinen J, Anttila A, Holmburg K, Hirvinen JP (1992) Diam Relat Mater 1:639
123. Ferrari AC, Robertson J (2000) Phys Rev B 61:14095
124. Ferrari AC, Robertson J (2001) Phys Rev B 64:075414
125. Tiainen VM (2001) Diam Relat Mater 10:153
126. Lappalainen R, Heinonen H, Anttila A, Santavirta S (1998) Diam Relat Mater 7:482
127. Onate JI, Comin M, Braceras I, Garcia A, Viviente JL, Brizuela M et al (2001) Surf Coat Technol 142–144:1056
128. Dong H, Shi W, Bell T (1999) Wear 225–229:146
129. Sheeja D, Tay BK, Shi X, Lau SP, Daniel C, Krishnan SM (2001) Diam Relat Mater 10:1043
130. Dowling DP, Kola PV, Donelly K, Kelly TC, Brumitt K, Lloyd L et al (1997) Diam Relat Mater 6:390
131. Sheeja D, Tay BK, Lau SP, Nung LN (2001) Surf Coat Technol 146–147:410

132. Saikko V, Ahlroos T, Calonius O, Keraen J (2001) J Biomater 22:1507
133. Affatato S, Frigo M, Toni A (2000) J Biomed Mater Res 53:221
134. Ahlroos T, Saikko V (1997) Wear 211:113
135. Liao YS, McNulty D, Hanes M (2003) Wear 255:1051
136. Saikko V, Ahlroos T (1997) Wear 207:86
137. Fisher J, Firkins P, Reeves EA, Hailey JL, Isaac GH (1995) Proc Inst Mech Eng H J Eng Med 209:263
138. Ronkainen H, Varjus S, Holmberg K (2001) Wear 249:267
139. Platon F, Fournier P, Rouxel S (2001) Wear 250:227
140. Shi B, Ajayi OO, Fenske G, Erdemir A, Liang H (2003) Wear 255:1015
141. Kim SK, Lee JB, Koak JY, Heo SJ, Lee KR, Cho LR, Lee SS (2005) J Oral Rehabil 32(5):346
142. Lappalainen R, Selenius M, Anttila A, Konttinen YT, Santavirta SS (2003) J Biomed Mater Res B Appl Biomater 66B:410
143. Ronkainen H, Likonen J, Koskinen J, Varjus S (1996) Surf Coat Technol 79:87
144. Neerinck D, Persoone P, Sercu M, Goel A, Venkatraman C, Kester D et al (1998) Thin Solid Films 317:402
145. Taeger G, Podleska LE, Schmidt B, Ziegler M, Nast-Kolb D (2003) Mat-wiss u Werkstofftech 34:1094
146. Chandra L, Allen R, Butter M, Rushton N, Lettington AH, Clyne TW (1995) J Mater Sci Mater Med 6:581
147. Muller U, Hauert R, Oral B, Tobler M (1995) Surf Coat Technol 71:233
148. Puértolas JA, Martínez-Nogués V, Martínez-Morlanes MJ, Mariscal MD, Medel FJ, López-Santos C, Yuberoc F (2010) Wear 269:458
149. Kvasnica S, Schalko J, Benardi J, Eisenmenger-Sittner C, Pauschitz A, Roy M (2006) Diam Relat Mater 15:1743
150. Ali N, Kousar Y, Okpalugo TI, Singh V, Pease M, Ogwu AA, Gracio J, Titus E, Meletis EI, Jackson MJ (2006) Thin Solid Films 515:59
151. Grischke M, Bewilogua K, Trojan K, Demigen H (1995) Surf Coat Technol 74–75:739
152. Memming R (1986) Thin Solid Films 143:279
153. Choe HC, Chung CH, Brantley W (2007) Key Eng Mater 345–346:1201
154. Jung SW, Son MK, Chung CH, Kim HJ (2009) J Adv Prosthodont 1(2):102
155. Gispert MP, Serro AP, Colaco R, Botelho do Rego AM, Alves E, da Silva RC, Brogueira P, Pires E, Saramago B (2007) Wear 262:1337
156. Wang L, Su JF, Nie X (2010) Surf Coat Technol 205:1599
157. Serro AP, Completo C, Colaço R, dos Santos F, Lobato da Silva C, Cabral JMS, Araújo H, Pires E, Saramago B (2009) Surf Coat Technol 203:3701
158. Hoseini M, Jedenmalm A, Boldizar A (2008) Wear 264:958
159. Osterle W, Klaffke D, Griepentrog M, Gross U, Kranz I, Knabe C (2008) Wear 264:505
160. Gulhane UD, Roy M, Sapate SG, Mishra SB, Mishra PK (2009) In: Proceedings of ASME/STLE International Joint Tribology Conference, IJTC 2009, October 19–21, Memphis, TN
161. Roy M, Koch T, Pauschitz A (2010) Adv Surf Sci 256:6850
162. Unsworth A (1991) J Eng Med 205:163
163. Zhu X, Eibl O, Scheider L, Geis-Gerstofer J (2006) J Biomed Mater Res 79A:114
164. Liao SS, Cui FZ, Zhang W, Feng QL (2004) J Biomed Mater Res B Appl Biomatter 69(2):158
165. Pezzatini S, Solito R, Morbidelli L et al (2006) J Biomed Mater Res 76A:656
166. Rajtar A, Kaluza GL, Yang Q et al (2006) EuroIntervention 2:113
167. Campbell AA (2003) Mater Today 11:26
168. Balani K, Anderson R, Lahaa T et al (2007) Biomaterials 28:618